Journal of Low Temperature Physics, Vol. 46, Nos. 1/2, 1982

Third Sound and Thermal Conduction in Thin ^{4}He Films*

S. Teitel†

Laboratory of Atomic and Solid State Physics, Cornell University, Ithaca, New York

(Received April 22, 1981; revised July 28, 1981)

The dynamic Kosterlitz–Thouless theory of superfluidity in two dimensions is applied to the problems of third-sound propagation and thermal conduction in thin ^{4}He films. Extensions of existing theory are made and the results are compared with experiment.

1. INTRODUCTION

In a recent paper[1] (henceforth referred to as AHNS) the static Kosterlitz–Thouless picture of superfluidity in two dimensions[2–4] has been generalized to describe dynamic processes in thin ^{4}He films. A detailed comparison between this dynamic theory and data from torsional oscillator experiments has shown good agreement.[5] In AHNS, the authors also make certain predictions regarding the propagation of third sound and thermal conduction in thin films. In this paper we discuss the theory of these last two phenomena in somewhat more detail, and make comparisons with available experimental data.

In Section 2 we deal with the phenomenon of third sound. In Section 2.1 we review the results of AHNS, who calculate third-sound velocity and damping neglecting mass flow out of the film to the vapor phase and assuming isothermal propagation. We show that, close to the critical temperature, relaxing the above assumptions does not alter the main features of the above model. In Section 2.2 we make comparison with published third-sound data.

In Section 3 we deal with the phenomenon of steady-state heat conduction. In Section 3.1 we extend the prediction of AHNS to a particular experimental geometry and calculate thermal resistivity. For the geometry

*This work was supported by the National Science Foundation under Grant No. DMR-77-18329.

†Present address: Department of Physics, The Ohio State University, Columbus, Ohio.

0022-2291/82/0100-0077$03.00/0

considered, the effect of viscous flow in the vapor phase is seen to be the limiting factor in thermal resistivity at low temperatures. In Section 3.2 a comparison is made with the results of Section 3.1 and some preliminary experimental data. Our conclusions are presented in Section 4.

2. THIRD SOUND

2.1. Theoretical Results

The problem of third sound in both thin and thick films has been extensively studied within the context of standard two-fluid hydrodynamics by Bergman[6,7] and more recently by Verbeek.[8] Close to the Kosterlitz–Thouless transition temperature, however, effects due to the motion of vortices become important and the standard two-fluid hydrodynamics must be modified.

We imagine a film on a substrate in contact with a vapor phase above it as in Fig. 1. The required modification, as given by AHNS, yields the following hydrodynamic equations [AHNS, Eqs. (5.10)–(5.12)][1]:

$$\partial \mathbf{v}_s/\partial t = \bar{S}\nabla T - f\nabla h - \hat{\mathbf{z}}\times \mathbf{J}_v \tag{1}$$

$$\partial(\bar{\rho}h)/\partial t = -\rho_s^0 \nabla \cdot \mathbf{v}_s - J_m \tag{2}$$

$$\bar{\rho}hC\,\partial T/\partial t = \rho_s^0 T\bar{S}\nabla \cdot \mathbf{v}_s + \kappa h\nabla^2 T - LJ_m - J_{Qg} - J_{Q\text{sub}} \tag{3}$$

Here $\mathbf{v}_s$ is the "semimicroscopic" superfluid velocity as defined in AHNS and ρ_s^0 the bare superfluid density per unit area. Equations (2) and (3) are Bergman's equations for mass conservation and heat flow. The height of the film is h, T is the temperature, $\bar{\rho}h$ is the total mass density

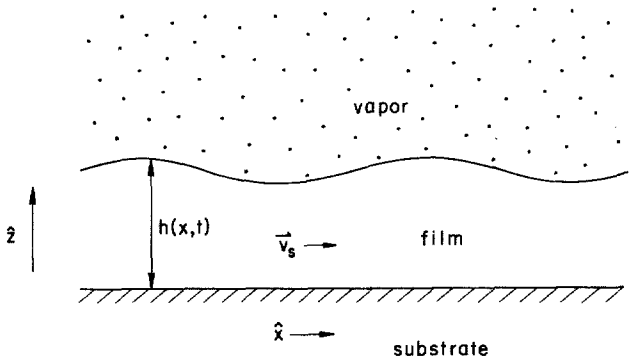

Fig. 1. Geometry of a third-sound wave.

per unit area, C is the specific heat per unit mass, κ is the thermal conductivity (in the local rest frame) of the helium in the film, $\bar{S} = \partial S/\partial M$ is the partial entropy per unit mass (M is the total mass of a film with constant area), and L is the latent heat of evaporation per unit mass from the film to the vapor. J_m is the mass flow per unit area from the film to the vapor, and J_{Qg} and $J_{Q\text{sub}}$ are the heat currents from the film to vapor and substrate, respectively.

Equation (1) is the necessary modification of the Josephson equation for superfluid motion in the presence of vortices. The right-hand side of (1) consists of two pieces. The first is the gradient of the chemical potential of the film μ_f, which serves to drive the superfluid flow,

$$-\nabla\mu_f = \bar{S}\nabla T - f\nabla h \tag{4}$$

where f is the van der Waals force constant.

The second piece, $\hat{\mathbf{z}}\times\mathbf{J}_v$, is a vortex current perpendicular to the direction of superfluid flow, which serves to dissipate the flow. $\mathbf{J}_v$ is given by [AHNS, Eq. (5.4)][1]

$$\mathbf{J}_v(\mathbf{r}, t) = \frac{2\pi\hbar}{m}\sum_i n_i \frac{d\mathbf{r}_i(t)}{dt}\,\delta(\mathbf{r}-\mathbf{r}_i(t)) \tag{5}$$

$\mathbf{r}_i$ are the positions of the discrete set of vortices, and $n_i = \pm 1$ their strengths. If we average $\mathbf{J}_v$ over an area small compared to the size of the wavelength of our third-sound wave, then the main result of AHNS, Section V, gives for the longitudinal (i.e., curl-free) part of this average $\hat{\mathbf{z}}\times\mathbf{J}_v$,

$$-(\hat{\mathbf{z}}\times\mathbf{J}_v)_L = [1-\varepsilon(\omega)]\, d\mathbf{v}_L/dt \tag{6}$$

where $\mathbf{v}_L$ is the longitudinal part of $\mathbf{v}_s$, and $\varepsilon(\omega)$ is the dynamic dielectric function, which describes the effective screening due to vortices. Combining (6) with (1) gives

$$\varepsilon(\omega)\,\partial\mathbf{v}_L/\partial t = \bar{S}\nabla T - f\nabla h \tag{7}$$

The transverse part of $\mathbf{v}_s$ decouples from the other equations and gives a purely relaxational mode. To solve Eqs. (7), (2), and (3), AHNS make the approximations $J_m = 0$ and $\nabla T = 0$. In this case, Eqs. (7) and (2) decouple from (3) and we can easily solve for the resulting complex third-sound velocity c_3

$$c_3^2 = c_0^2/\varepsilon(\omega) \tag{8}$$

where c_0 is the unrenormalized isothermal sound velocity

$$c_0^2 = f\rho_s^0/\rho \tag{9}$$

and $\rho = \bar{\rho} + h\, d\bar{\rho}/dh$ is the total mass density of the film per unit volume evaluated at the film–vapor interface.

To deal with the more general case where J_m, $\nabla T \neq 0$ we make the following observation. If we define the renormalized superfluid density as

$$\rho_s(\omega) = \rho_s^0/\varepsilon(\omega) \tag{10}$$

and the macroscopic superfluid velocity as

$$\mathbf{V}_s = \varepsilon(\omega)\mathbf{v}_L \tag{11}$$

and note that $\nabla \cdot \mathbf{v}_s = \nabla \cdot \mathbf{v}_L$, then we may write Eqs. (7), (2), and (3) in the standard two-fluid model form,

$$\partial \mathbf{V}_s/\partial t = \bar{S}\nabla T - f\nabla h \tag{12a}$$

$$\partial(\bar{\rho}h)/\partial t = -\rho_s(\omega)\nabla \cdot \mathbf{V}_s - J_m \tag{12b}$$

$$\bar{\rho}hC\, \partial T/\partial t = \rho_s(\omega)T\bar{S}\nabla \cdot \mathbf{V}_s + \kappa h\nabla^2 T - LJ_m - J_{Qg} - J_{Q\text{sub}} \tag{12c}$$

These equations are now identical to Bergman's if we identify his $h\bar{\rho}_s$ with our $\rho_s(\omega)$. It is now easy to see that the solutions to the general equations (12) have the same form as the model of AHNS[1] [Eq. (2.8)].

Bergman solves Eqs. (12) for the case of a fixed frequency ω and a semi-infinite substrate and vapor below and above the film, respectively, a geometry applicable to the experiments of Rudnick.[9–11] In his expression for the dispersion relation which determines c_3 [Eq. (53) of Ref. 6] the areal superfluid density and sound velocity enter only in the ratio ρ_s/c_3^2. (Actually there is also a term B given by $B^{-1} = B_1^{-1} + (\kappa_{\text{sub}}q)^{-1}$, where κ_{sub} is the thermal conductivity of the substrate, B_1 is the Kapitza conductance between film and substrate, and $q^2 = k^2 - i\omega C_{p\text{sub}}/\kappa_{\text{sub}}$ is the thermal wave vector of the substrate. $C_{p\text{sub}}$ is the specific heat of the substrate per unit volume at constant pressure, and $k = \omega/c_3$ is the wave vector of the third-sound wave. For the experiments of interest, however, one can show that this k dependence in q and hence B is negligible.)

Thus, noting our definition for ρ_s in Eq. (10), we have the general result in analogy with Eq. (8)

$$c_3^2 = c^2(T)/\varepsilon(\omega) \tag{13}$$

where $c(T)$ is a smooth, slowly varying, and in general complex function throughout the transition region. That $c(T)$ is smooth follows from the fact that all thermodynamic functions of the film show no divergent behavior as we pass through the Kosterlitz–Thouless transition temperature.[12]

For a different geometry than that considered above, we still expect the dominant part of c_3 to go like $c_3^2 \sim \rho_s$, and hence we still expect an equation of the form (13) to be a good description in the transition region.

The quantities of experimental interest are the real third-sound velocity and the Q factor, which is a measure of the damping. For a wave of fixed frequency ω and wave vector $k = \omega/c_3$ we have

$$u_3 = \omega/\mathrm{Re}\,(k) \tag{14a}$$

$$Q = \tfrac{1}{2}\,\mathrm{Re}\,(k)/\mathrm{Im}\,(k) \tag{14b}$$

The behavior of $\varepsilon(\omega)$ is discussed in AHNS[1] and Appendix A of Ref. 5. It is found to have an imaginary part which increases rapidly due to the production of free vortices as T increases above T_c. In the transition region, therefore, the dominant imaginary part of c_3 is due to ε and for $\mathrm{Re}\,c_3 \gg \mathrm{Im}\,c_3$ (which must be true to still have a propagating third-sound mode) we have

$$u_3 \cong \mathrm{Re}\,c(T)/[\mathrm{Re}\,\varepsilon(\omega)]^{1/2} \tag{15a}$$

$$Q \cong \mathrm{Re}\,\varepsilon(\omega)/\mathrm{Im}\,\varepsilon(\omega) \tag{15b}$$

2.2. Comparison with Experiment

We now compare the predictions of the previous section with experiment. In his analysis, Bergman tried to fit his model to the data of Rudnick *et al.*,[9-11] who measure third-sound velocity and attenuation as a function of film thickness for a fixed temperature. Since our model involves $\varepsilon(\omega)$, which we know as a function of temperature but not of thickness, quantitative comparison with these experiments is difficult. However, the following general feature is clear. $\varepsilon(\omega)$ depends on the thickness h through the critical temperature $T_c(h)$, which decreases as h decreases. Since $\varepsilon(\omega, h)$ will depend on $T_0 - T_c(h)$, where T_0 is the fixed temperature of the experiment, as h decreases, eventually $T_c(h)$ drops below T_0, the imaginary part of $\varepsilon(\omega)$ rapidly increases, and the third-sound mode will damp out. This qualitatively explains the onset phenomenon seen in these experiments where there is a minimum thickness required for third sound to propagate.

By looking at the third-sound velocity at the onset thickness for various temperatures, Rudnick[13] is able to estimate the universal jump[4] $\rho_s(T_c)/T_c$ and obtains a value of $(3.30 \pm 0.21) \times 10^{-9}$ (as compared to the theoretical 3.49×10^{-9}). We may analyze the expected accuracy of such an estimate as follows. Using Bergman's expression for the third-sound velocity, we can write

$$u_3^2 = \frac{\rho_s^0 f}{\mathrm{Re}\,[\varepsilon(\omega)]\rho}\left(1 + \frac{T\bar{S}}{L}\right) \tag{16}$$

This is just Eq. (8) with c_0 modified by the factor $(1 + T\bar{S}/L)$ due to the film–vapor interaction. The results of AHNS[1] for $\varepsilon(\omega)$ (see also

Appendix A of Ref. 5) give

$$\mathrm{Re}\,[\varepsilon(\omega)]=\frac{\rho_s^0}{\rho_s(T_c^-)}\,\frac{T_c}{T}\left[1-\frac{1}{2}x(l)\right] \tag{17}$$

where

$$\begin{aligned} x(l)&=\begin{cases} x_0\coth(x_0 l), & T<T_c \\ x_0\cot(x_0 l), & T>T_c \end{cases} \\ x_0&=\tfrac{1}{2}b(|T-T_c|/T_c)^{1/2} \end{aligned} \tag{18}$$

$l=\frac{1}{2}\ln(14D/a_0^2\omega)$ is the dynamic length scale, and b is the nonuniversal parameter describing the square root cusp in the static renormalized ρ_s. Substituting this expression for $\varepsilon(\omega)$ into Eq. (16) yields

$$\frac{\rho_s(T_c^-)}{T_c}=\left(1-\frac{x(l)}{2}\right)\frac{u_3^2(T)\rho}{Tf(1+T\tilde{S}/L)} \tag{19}$$

In particular, as $x(l)=0$ for $T=T_c$, we can evaluate (19) at $T=T_c$ to get

$$\frac{\rho_s(T_c^-)}{T_c}=\frac{u_3^2(T_c)\rho_f}{T_c f(1+T\tilde{S}/L)} \tag{20}$$

and thus extract the jump directly from the third-sound velocity at T_c.

However, as the third-sound mode continues to propagate above T_c, the identification of T_c from the measured u_3 without a detailed fit to the data involves some guesswork. Comparing (19) with (20), we see that the fractional error introduced in the jump from applying (20) at some T close to but not equal to T_c is given by

$$\tfrac{1}{2}x(l,(T-T_c)/T) \tag{21}$$

where we explicitly display the T dependence of x.

In Rudnick's experiments the same problem exists in determining the critical thickness h_c such that $T_0=T_c(h_c)$, where T_0 is the fixed temperature of the experiment. If, in evaluating (20), one uses values at an onset thickness h_0 (experimentally determined as the thickness at which the signal is lost), which is in fact somewhat lower than h_c, then the fractional error induced is again

$$\tfrac{1}{2}x(l,[T_0-T_c(h_0)]/T_0) \tag{22}$$

As the difference h_c-h_0 increases, the error will rapidly increase due to the rapid increase in $x(l)$ as T increases above T_c [see Eq. (18)]. One must, therefore, be very careful in making estimates based on an eyeball determination of T_c (or equivalently h_c).

For a more quantitative comparison with experiment we turn to the measurements of Ratnam and Mochel,[14] who measure sound velocity as a function of temperature for film thicknesses on the order of one monolayer. In Fig. 2 we show a plot of data from Ref. 14 of third-sound velocity u_3 versus temperature. Our calculated u_3 is fit to the data in Fig. 2 in a manner similar to that described in Appendix A of Ref. 5. A constant Re $c(T)$ for Eq. (15a) is adjusted to give the correct velocity at $T = 1.24$ K. In principle one could try and calculate $c(T)$ by knowing the thickness and thermodynamic functions of the film. Unfortunately, sufficient information was not available to do so. The parameter l used was the same found to fit the torsional oscillator experiments, appropriately scaled to the proper frequency (see Appendix A of Ref. 5). The fit yields the values of the remaining parameters $T_c = 1.2515$ K, $b = 5.44$. Note that the value for b is very close to the value of 5.5 found for the torsional oscillator experiments.[5]

Turning now to the damping of the third-sound wave, we have already noted how the rapid rise in the imaginary part of $\varepsilon(\omega)$ will give rise to the onset phenomena seen by Rudnick. For a fixed thickness and varying temperature, Eq. (15b) predicts a rapid drop in the Q as T goes above T_c. In Ref. 15, Ratnam and Mochel see such an effect. Their data, however, are not sufficiently detailed to try a quantitative fit based on Eq. (15b).

Finally we remark on the damping of third sound outside the critical region (i.e., $T \ll T_c$ or $h \gg h_c$). In this limit, we believe the vortices to be bound together into tight pairs and therefore to produce negligible effects. We have $\varepsilon(\omega) \to 1$ and the damping is due entirely to the complex part of $c(T)$, which one computes from the usual two-fluid model. Such calculations, however, seem to be in poor agreement with experiment.[8,9,16,17]

A similar disagreement is seen in the torsional oscillator experiments for helium on Mylar,[5] where there is unexplained dissipation at low temperatures. If one supposes the origin of this dissipation to arise from complications in vortex motion due to substrate inhomogeneities resulting

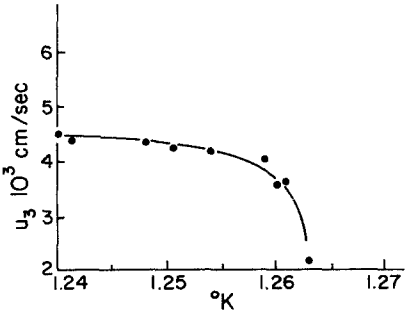

Fig. 2. Third-sound velocity u_3 versus temperature for Re $(k) = 1.653$ cm^{-1}. The solid line is a fit to the data using Eq. (15a). The fit determines $T_c = 1.2515$ K, $b = 5.44$. (Data from Ref. 14.)

in a nonnegligible Im $\varepsilon(\omega)$ below T_c, then one can estimate the equivalent dissipation to be expected in third sound on a Mylar substrate. Comparing Eq. (15b) with Eq. (A4) of Ref. 5, we can relate the Q of the torsional oscillator (Q^{BR}) to the expected Q of the third sound ($Q^{3\mathrm{S}}$) by $Q^{3\mathrm{S}} = (A\rho_s/M)Q^{\mathrm{BR}}$, where A is the surface area and M the mass of the oscillator and $\rho_s \equiv \rho_0/\mathrm{Re}\,\varepsilon$. Using the value from Ref. 5 of $A\rho_s/M \simeq 4\times10^{-6}$ and the measured low-temperature value $Q^{\mathrm{BR}} \simeq 3\times10^6$, we would estimate $Q^{3\mathrm{S}} \simeq 10$. This compares with the low-temperature value $Q^{3\mathrm{S}} \simeq 10^4$ seen by Ratnam and Mochel,[15] who, however, use an argon-coated glass substrate. Thus, either such vortex effects greatly depend upon the substrate or geometry of a particular experiment, or the origin of the failure of the theory is different in the two cases.

3. THERMAL CONDUCTION

3.1. Theoretical Description

Consider an experimental cell such as in Fig. 3. Helium is deposited on the inner walls of the substrate and vapor fills the gap in between. A heater applies a steady power at one end and the temperature jump ΔT across the cell is measured. To solve for the problem of heat conduction in the film we use the steady state versions of the hydrodynamic equations (1)–(3):

$$\hat{\mathbf{z}}\times\mathbf{J}_v = -\nabla\mu_f \tag{23}$$

$$\rho_s^0 \nabla\cdot\mathbf{v}_s + J_m = 0 \tag{24}$$

$$(L + T\bar{S})J_m + J_{Qg} + J_{Q\mathrm{sub}} - \kappa_f h\nabla^2 T = 0 \tag{25}$$

where (25) follows from substituting (24) into (3). Here $\hat{\mathbf{z}}\times\mathbf{J}_v$ and $\mathbf{v}_s$ are to be viewed as being local averages over vortex positions of the respective semimicroscopic quantities.

For the situation of Fig. 3, we expect a constant temperature gradient $\nabla T = \Delta T/W$, hence $\nabla^2 T = 0$. The thermal current into the substrate $\mathbf{J}_{Q\mathrm{sub}}$ is determined by the Kapitza conductance B_1, i.e., $J_{Q\mathrm{sub}} = B_1(T_{\mathrm{film}} - T_{\mathrm{sub}})$. For a steady state situation we must have $T_{\mathrm{film}} = T_{\mathrm{sub}}$ and hence $J_{Q\mathrm{sub}} = 0$. Finally, since both J_{mg} and J_{Qg} must be of the same sign (J_{mg} being proportional to $\langle m\mathbf{v}_g\rangle$ and J_{Qg} being proportional to $\langle\frac{1}{2}mv_g^2\mathbf{v}_g\rangle$, where the average is over velocities $\mathbf{v}_g$ of gas atoms at the interface), there is no way to satisfy (25) unless $J_{mg} = J_{Qg} = 0$. Hence from (24) we have $\nabla\cdot\mathbf{v}_s = 0$ and $\mathbf{v}_s$ is a constant.

The process we have, therefore, is a constant flow in the film from the cold to the hot end. Upon hitting the hot end, helium is evaporated. A

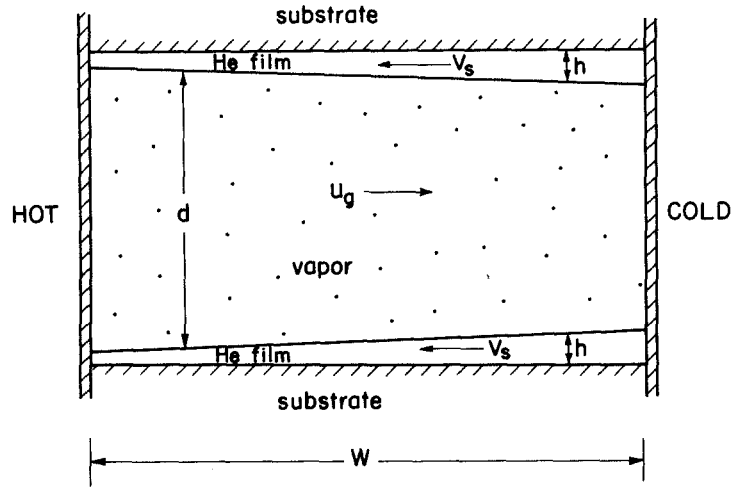

Fig. 3. Geometry of a model heat conduction cell. W is the width of the cell from hot to cold ends. $\mathscr{L}$ is the cell length in contact with the heater perpendicular to the page.

counter mass flow in the gas flows to the cold end, where helium condenses back to the film.

Since we have $J_{mg} = 0$, film and gas are in equilibrium and hence their chemical potentials must be equal. We may therefore write (23) as

$$\hat{\mathbf{z}} \times \mathbf{J}_v = -\nabla \mu_g = s_g \nabla T - (1/\rho_g) \nabla P \tag{26}$$

where s_g and ρ_g are the entropy per unit mass and density of the gas. P is the pressure in the gas.

A pressure gradient will produce a mass flow in the gas down the channel between film layers (see Fig. 3). If the mean free path l of molecules in the gas is much less than the thickness d of the channel, then the gas flow is determined by hydrodynamics. Since $\mathbf{v}_n = 0$ in the film, the gas will be viscously clamped to the film at the interface, and we have what is known as Poiseuille flow. The average flow velocity of the gas is easily found to be[18]

$$\mathbf{u}_g = -\frac{d^2}{12} \frac{\nabla P}{\eta} \tag{27}$$

where $\eta \approx \frac{1}{3} \rho_g \bar{v} l$ is the shear viscosity of the gas[19] [$\bar{v} = (8 k_B T / \pi m)^{1/2}$ is the mean atomic speed].

If we are in the limit $l \gg d$, then it has been shown that the form (27) is still valid provided we take as the effective viscosity[20]

$$\eta = \frac{5\pi}{12 \cdot 8} \frac{4}{5} \rho_g \bar{v} d \left(\ln \frac{2.089 l}{d} \right)^{-1} \tag{28}$$

We now balance the mass flows in the gas and the film,

$$\tfrac{1}{2} \rho_g \, du_g = -\rho_s^0 v_s \tag{29}$$

where the factor $\frac{1}{2}$ arises as half the mass from the gas condenses into each of the two layers of film (see Fig. 3).

Combining Eq. (29) with (27) yields

$$\frac{1}{\rho_g} \nabla P = \rho_s^0 \mathbf{v}_s \frac{24\eta}{\rho_g^2 d^3} \tag{30}$$

and eliminates the unknown ∇P in favor of the variable $\mathbf{v}_s$.

Finally we need an expression for $\hat{\mathbf{z}} \times \mathbf{J}_v$. Since $\mathbf{v}_s$ is a constant, ∇P is a constant and hence so is $\nabla \mu_f$. We may thus average Eq. (26) over the area A of the film. The areal average of $\hat{\mathbf{z}} \times \mathbf{J}_v$ is easily obtained from the definition of $\mathbf{J}_v$, Eq. (5). We get

$$\langle \hat{\mathbf{z}} \times \mathbf{J}_v \rangle \equiv \int \frac{d^2 r}{A} (\hat{\mathbf{z}} \times \mathbf{J}_v) = \frac{2\pi\hbar}{Am} \left\langle \sum_{i,\text{free}} n_i \hat{\mathbf{z}} \times \frac{d\mathbf{r}_i}{dt} \right\rangle + \frac{2\pi}{A} \frac{\hbar}{m} \left\langle \sum_{\alpha,\text{bound}} \hat{\mathbf{z}} \times \frac{d\mathbf{r}_\alpha}{dt} \right\rangle \tag{31}$$

where the first sum is over free vortices located at positions $\mathbf{r}_i$ and the second sum is over bound pairs with dipole moments $\mathbf{r}_\alpha = (\mathbf{r}_+ - \mathbf{r}_-)$, and angular brackets indicate an average over vortex positions.

The contribution due to the free vortices is easily calculated by using the equation of motion for vortices [AHNS,[1] Eq. (2.6)]

$$\frac{d\mathbf{r}_i}{dt} = n_i \frac{D 2\pi\hbar\rho_s^0}{m k_B T} \hat{\mathbf{z}} \times (\mathbf{v}_n - \mathbf{v}_s^i) + C(\mathbf{v}_n - \mathbf{v}_s^i) + \mathbf{v}_s^i + \boldsymbol{\eta}_i \tag{32}$$

and noting that for a free vortex at $\mathbf{r}_i$, the average of the semimicroscopic superfluid velocity $\mathbf{v}_s^i$ at $\mathbf{r}_i$ is just $\mathbf{v}_s$. Assuming $\sum_i n_i = 0$, we get

$$\langle \hat{\mathbf{z}} \times \mathbf{J}_v \rangle_{\text{free}} = (2\pi\hbar/m)^2 (D/k_B T) \rho_s^0 \mathbf{v}_s n_f \tag{33}$$

where D is the diffusion constant for vortices and $n_f = A^{-1} \sum_i n_i^2$ is the density of free vortices. These free vortices may be due to thermal activation above T_c or due to the escape of bound pairs over the potential barrier set up by the steady state v_s (see Section IV of AHNS[1]).

The contribution to $\langle \hat{\mathbf{z}} \times \mathbf{J}_v \rangle$ from bound pairs has been ignored in the literature. We believe this piece to be in general nonzero, but argue in Appendix A that it is negligible compared to the free vortex contribution (33).

We now combine our expression (33) for $\langle \hat{\mathbf{z}} \times \mathbf{J}_v \rangle$ and the expression (30) for ∇P with the steady state Josephson equation (26) to get

$$\rho_s^0 v_s \left[\left(\frac{2\pi\hbar}{m} \right)^2 \frac{D}{k_B T} n_f + \frac{24\eta}{\rho_g^2 d^3} \right] = s_g \nabla T \tag{34}$$

Equation (34) tells us the relative importance of thermal resistance in the film and the gas. In order to see the effects of resistance due to vortices, we must have a density of free vortices large enough that

$$n_f = \frac{24\eta}{\rho_g^2 d^3} \left(\frac{m}{2\pi\hbar} \right)^2 \frac{k_B T}{D} \tag{35}$$

Thus for a good experiment we want to minimize the right-hand side of Eq. (35) (one may take a very large d, for example).

The power absorbed by the film in the heat conduction process is the energy needed to evaporate the helium from the film to the gas as it hits the hot end of the cell. This power is

$$\mathscr{P}_f = 2L\mathscr{L}\rho_s^0 v_s \tag{36}$$

where L is the latent heat of evaporation, $\mathscr{L}$ is the length of the film in contact with the heater, and the factor 2 is from the two layers of film in the cell.

We now consider an idealized experiment where we can ignore the effects of the gas. This is the limit dealt with in AHNS. Equation (34) then becomes

$$v_s n_f \propto \nabla T \tag{37}$$

Below T_c, n_f is due entirely to the splitting of vortex pairs by escape over the potential barrier created by the constant flow v_s. In AHNS,[1] Section IV, the density of such free vortices is computed. For $T < T_c$ but not too close to T_c it is shown that [AHNS,[1] Eq. (4.19)]

$$n_f \simeq \frac{b\sqrt{|t|}}{a_0^2} \left(\frac{a_0}{r_c} \right)^{2+(b/2)\sqrt{|t|}} \tag{38}$$

where $r_c \simeq \hbar/mv_s\tilde{\varepsilon}(r_c)$ is the critical pair separation which locates the saddle point in the potential energy $U(r)$ for a pair of separation $\mathbf{r}$. Here $\tilde{\varepsilon}$ is the static Kosterlitz–Thouless dielectric function, a_0 is the core size of the vortex, b is the nonuniversal parameter introduced in Eq. (18), and

$t = |T - T_c|/T_c$ is the reduced temperature. Combining Eq. (38) with (37) and inserting in (36), we find for the temperature jump across the cell ΔT

$$\Delta T \propto \mathscr{P}_f^{\gamma} \tag{39}$$

where

$$\gamma = 3 + \tfrac{1}{2} b\sqrt{|t|} = 1 + \rho_s(T)/\rho_s(T_c^-) \tag{40}$$

and ρ_s is the static renormalized superfluid density.[4]

Above T_c we have thermally activated free vortices whose density is given by AHNS,[1] Eq. (3.23) as

$$n_f \sim \xi_+^{-2} = a_0^{-2} \exp(-4\pi/b\sqrt{|t|}) \tag{41}$$

We will also continue to have free vortices due to escape of pairs over the potential barrier, provided $r_c \ll \xi_+$. Once $r_c \simeq \xi_+$, the average separation of free vortices, it no longer makes sense to consider a pair on this length scale and the entire free vortex density is due to (41). Combining (41) with (37) and (36), we have in this region

$$\Delta T \propto \mathscr{P}_f \tag{42}$$

This change from a linear to a power law relation between $\mathscr{P}_f$ and ΔT, as first noted by Hess *et al.*,[23] provides one characteristic of the transition.

We return now to the more general results (34). Combining with Eq. (36), we have

$$\mathscr{P} = \Delta T\left(\kappa_{\text{cell}} + \frac{2Ls_g\mathscr{L}/W}{(2\pi\hbar/m)^2(D/k_B T)n_f + 24\eta/\rho_g^2 d^3}\right) \tag{43}$$

where $\mathscr{P}$ is the total power output of the heater and κ_{cell} is the conductivity due to any paths in parallel with the film gas system, such as conduction through the substrate or the container walls of the experimental cell. We define the thermal resistance of the cell as

$$R = \Delta T/\mathscr{P} \tag{44}$$

From (43) we see the following. At high temperatures as n_f rapidly increases, thermal conductivity is determined entirely by κ_{cell}. At low temperatures, where n_f gets small, thermal conductivity is determined by a combination of κ_{cell} and the viscous resistance offered by the gas. As n_f increases, we pass from one limit to the other.

3.2. Comparison with Experiment

We will now discuss a fit of Eq. (43) to some preliminary experimental data by Agnolet and Reppy.[21] This experiment consists of the same jellyroll

of Mylar in a torsional oscillator as in the experiments of Ref. 5, with the addition of a heater driving a thermal current along the axis of rotation. The helium in the cell remains constant while the temperature varies. The thermal part of the experiment may be modeled by the geometry of Fig. 3, where $\mathscr{L}$ is the total length of the rolled up Mylar and W is its width.

The data, and our fits to it, are shown in Fig. 4. The dissipation Q^{-1} and the period shift $2\Delta P/P_0$ of the torsional oscillator were fit according to the procedure discussed in Appendix A of Ref. 5. These fits yield values for the parameters of $T_c = 1.4255$ and $b = 5.4$. We then compute the thermal resistivity $R = \Delta T/\mathscr{P}$ from Eq. (43), using the above values for T_c and b to calculate n_f from Eq. (41). We have assumed for this fit that contributions to n_f due to the breakup of bound pairs escaping over the potential barrier [Eq. (38)] are negligible. We verify this assumption in Appendix B.

The fit to the resistivity R involves two additional parameters. κ_{cell} was chosen to agree with the high-temperature limit and gives a value consistent with the process of heat conduction through the metal walls of the cell container. The parameter $24\eta/\rho_g^2 d^3$ was chosen to fit to the low-temperature limit. s_g was taken to be the ideal gas value[19] and for L we assume that the entropy of the film is negligible, i.e., $L = Ts_g$.

In principle, one should be able to compute the parameter $24\eta/\rho_g^2 d^3$. However, uncertainty in the values of film height h and the van der Waals force constant for Mylar[22] prevent an exact determination.

An order of magnitude estimate, however, can be made as follows. Taking $h = 2.5$ layers, $\alpha = 27$ K (layers)$^{-3}$, and a saturated vapor pressure $P_0 = 2870$ dynes/cm^2, we have for $T = 1.4$ K

$$\rho_g = (P_0 m/k_B T)\exp(-\alpha/h^3 T) \approx 3\times 10^{-5}\ \text{g/cm}^3 \tag{45}$$

To compute η, we note that $l \simeq 1/n\sigma_0$, where n is the density of atoms in the gas and σ_0 is the collision cross section ($\sigma_0 \sim 10$ Å^2). This yields $l \simeq 2\times 10^{-4}$ cm as compared to $d \simeq 5\times 10^{-5}$ cm. We thus use Eq. (28) to compute the effective η for the $l \gg d$ limit, and find $\eta \simeq 8\times 10^{-7}$ P. Combining this with Eq. (45) for ρ_g gives

$$24\eta/\rho_g^2 d^3 \approx 10^{17}\ \text{cm}^2/\text{g sec} \tag{46}$$

which compares very favorably with the fitted value of 0.8×10^{17} cm^2/g sec.

Using this value, we can return to Eq. (35) and find that we do not expect to see the effects of thermal resistance due to vortices in the film until $n_f \approx 10^{10}$ cm^{-2}. This only occurs at a temperature considerably above T_c.

Turning back now to Fig. 4, we see that the increase in R sets in sooner and rises more gradually than our theoretical prediction. This would

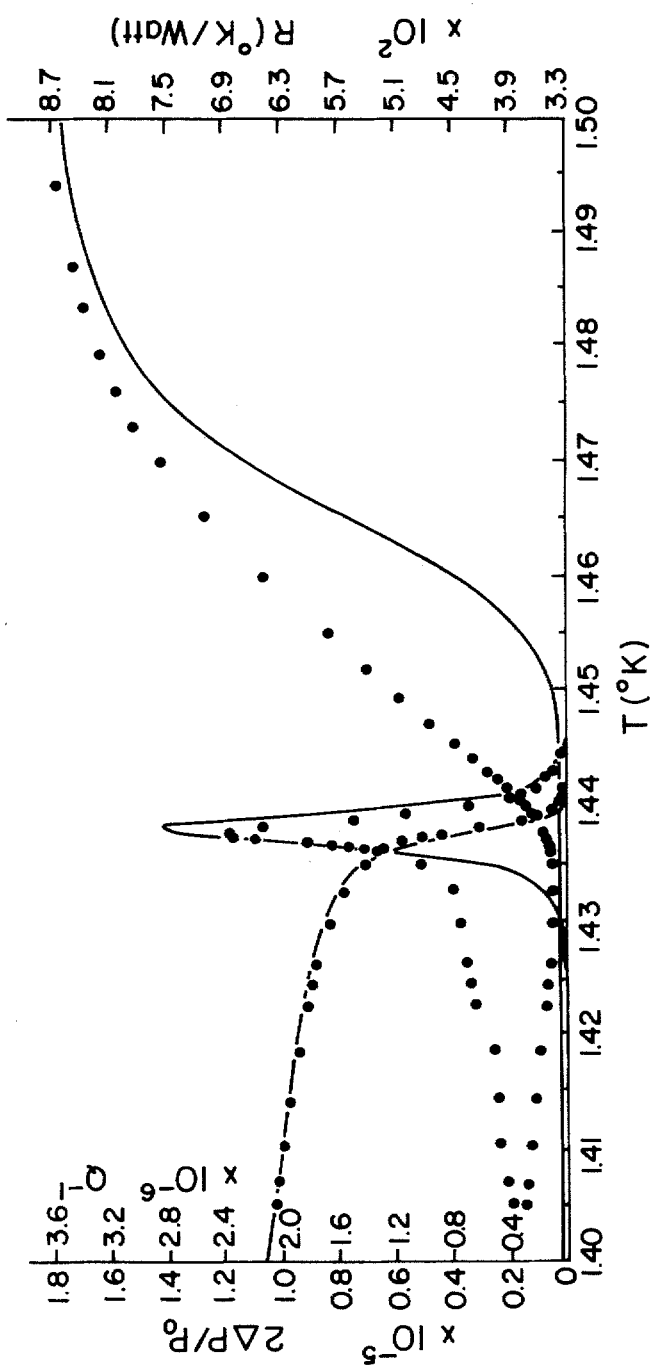

Fig. 4. Period shift $2\Delta P/P_0$, dissipation Q^{-1}, and thermal resistivity R in experiment of Agnolet and Reppy. Period shift and Q^{-1} are fit using the procedure of Appendix A of Ref. 5. This fit determines the parameters $T_c = 1.4255$ K, $b = 5.4$ for use in Eq. (43) to calculate R.

seem to indicate a higher density of free vortices sooner than Eq. (41) predicts. The fact, however, that both the theoretical and experimental curves saturate to the high-temperature limit at the same temperature is encouraging. As these data are only preliminary, we hope future experiments will help clarify the situation.[24,28]

4. CONCLUSIONS

In this paper we have extended the work of AHNS[1] in applying the dynamic Kosterlitz–Thouless theory of superfluidity to the phenomena of third sound and thermal conductivity in thin ^{4}He films.

We have considered a general model for third sound which includes the effects of mass and heat transport from the film to the surrounding media and demonstrated that close to the transition temperature the complex third-sound velocity retains the form predicted by the simpler model of AHNS. We have compared the results to a measurement of sound velocity versus temperature and found the fit to produce parameters consistent with torsional oscillator experiments.

The predictions concerning the dissipation of the third-sound mode appear qualitatively correct; however, no detailed measurements exist to allow a quantitative comparison. We hope that future experiments which make detailed measurements of both sound velocity and dissipation simultaneously as a function of temperature close to T_c will enable a better test of the theory.

We have also considered the problem of thermal conduction for a well-defined experimental geometry. In this model viscous flow in the vapor phase above the film is seen to be the limiting factor in the thermal conductivity at low temperatures. Comparison is made with some preliminary data. The low- and high-temperature limits of the measured thermal resistivity are consistent with the model. A torsional oscillator experiment done in parallel with the resistivity measurement allows an independent determination of the parameters necessary to compute the predicted resistivity in the transition region. Although the agreement between theory and experiment in this transition region is not as good as one would like, the fact that it occurs over roughly the correct temperature range with respect to T_c is encouraging. It is hoped that future experiments will help clarify the situation.

APPENDIX A

We wish to show that the contribution to $\langle \hat{\mathbf{z}} \times \mathbf{J}_v \rangle$ due to bound pairs may be neglected compared to the contribution from free vortices. If $\Gamma(\mathbf{r}, t)$

is the number of pairs per unit area with dipole moment $\mathbf{r}$, then Γ obeys the Fokker–Planck equation[25]

$$\frac{\partial \Gamma}{\partial t} = 2D\nabla \cdot \left(\frac{1}{k_B T} \frac{\partial U}{\partial \mathbf{r}} \Gamma + \frac{\partial \Gamma}{\partial \mathbf{r}} \right) \equiv \nabla \cdot \mathbf{j} \tag{A1}$$

where $U(\mathbf{r})$ is the energy of a pair with dipole moment $\mathbf{r}$. Here $\mathbf{j}$ is a density current describing the average movement of the pairs. The dipole moment of a given pair moves according to the Langevin equation[25]

$$\frac{d\mathbf{r}}{dt} = \frac{-2D}{k_B T} \frac{\partial U}{\partial \mathbf{r}} + \boldsymbol{\eta} \tag{A2}$$

where $\boldsymbol{\eta}$ is a fluctuating Gaussian noise term.

For the case of a steady $\mathbf{v}_s$ along the $\hat{\mathbf{x}}$ direction, $U(r)$ will have a saddle point at $\mathbf{r} = (0, r_c)$, where r_c is the critical pair separation $r_c \simeq \hbar / m v_s \tilde{\varepsilon}(r_c)$. Pairs are able to unbind by escaping over this saddle point (see AHNS,[1] Section IV) and we thus expect $\mathbf{j}$ to contain a nonzero current going over this potential barrier. r_c also represents the separation at which the velocity field at one member of the pair induced by the other member of the pair $[v = \hbar / m r \tilde{\varepsilon}(r)]$ becomes equal to the average imposed v_s.

We now imagine a closed contour C in the $\mathbf{r}$ plane, outside of which we consider the pair to be unstable. Such a contour is not precisely defined, but for concreteness we may imagine it to be a circle of radius r_c about the origin. The instability of the pair outside the contour C we represent by the boundary condition $\Gamma = 0$ along C.

The contribution to $\langle \hat{\mathbf{z}} \times \mathbf{J}_v \rangle$ from bound pairs is

$$\langle \hat{\mathbf{z}} \times \mathbf{J} \rangle_{\text{bound}} = \frac{2\pi\hbar}{m} \hat{\mathbf{z}} \times \int_C d^2 r \frac{d\mathbf{r}}{dt} \Gamma(\mathbf{r}, t) \equiv \frac{2\pi\hbar}{m} \hat{\mathbf{z}} \times \left\langle \frac{d\mathbf{r}}{dt} \right\rangle \tag{A3}$$

By making use of Eqs. (A1) and (A2), the boundary condition on Γ, and a partial integration, we can convert (A3) into the form

$$\langle \hat{\mathbf{z}} \times \mathbf{J}_v \rangle_{\text{bound}} = \frac{2\pi\hbar}{m} \hat{\mathbf{z}} \times \frac{d}{dt} \langle \mathbf{r} \rangle + \frac{2\pi\hbar}{m} \hat{\mathbf{z}} \times \oint_C dl\, \hat{\mathbf{n}} \cdot \begin{pmatrix} x\mathbf{j} \\ y\mathbf{j} \end{pmatrix} \tag{A4}$$

The first piece is zero, as Γ is a stationary distribution, i.e., $\partial \Gamma / \partial t = 0$. The second piece is a boundary integral along the contour C with $\hat{\mathbf{n}}$ the outward normal. We estimate the second piece by noting the following

contributions to $\mathbf{j}$ on the boundary C. First there is a piece $\mathbf{j}_{\text{escape}}$, primarily oriented in the positive $\hat{\mathbf{y}}$ direction, which represents the escape of bound pairs going over the potential barrier at $\mathbf{r} = (0, r_c)$. We estimate the contribution of this piece as

$$-(2\pi\hbar/m) r_c R \hat{\mathbf{x}} \tag{A5}$$

where

$$R = \oint_C dl\, \hat{\mathbf{n}} \cdot \mathbf{j}_{\text{escape}} \tag{A6}$$

is the escape rate of the bound pairs.

The second piece, $\mathbf{j}_{\text{recomb}}$, is due to the recombination of two free vortices into a bound pair as they pass within r_c of each other. The work of McCauley[26] suggests that to lowest orders in v_s, $\mathbf{j}_{\text{recomb}}$ is constant and points radially in toward the origin, thus giving no net contribution to the boundary integral in (A4). To next order in v_s, we expect a term of the same order of magnitude as (A5), which we expect to increase rather than cancel the contribution from escaping pairs (i.e., pairs will recombine preferentially by coming together from the negative $\hat{\mathbf{y}}$ side of the contour C, rather than coming back over the saddle point from the positive $\hat{\mathbf{y}}$ side).

To compare the estimated contribution to $\langle \hat{\mathbf{z}} \times \mathbf{J}_v \rangle$ from bound pairs

$$\langle \hat{\mathbf{z}} \times \mathbf{J}_v \rangle_{\text{bound}} \approx \frac{2\pi\hbar}{m} r_c R \hat{\mathbf{x}} \tag{A7}$$

with the contribution due to free vortices

$$\langle \hat{\mathbf{z}} \times \mathbf{J}_v \rangle_{\text{free}} = \left(\frac{2\pi\hbar}{m}\right)^2 \frac{D}{k_B T} \rho_s^0 \mathbf{v}_s n_f \tag{A8}$$

we note that a detailed balance argument gives a relation between the escape rate R and that part of n_f which we will call $\tilde{n}_f$, due to the unbinding of pairs (which is all of n_f for $T < T_c$).

This result as given by AHNS,[1] Eq. (4.18) is

$$R \approx \frac{\hbar^2}{m^2} \frac{D\rho_s^0}{k_B T} \frac{\tilde{n}_f^2}{\tilde{\varepsilon}(r_c)} \tag{A9}$$

Thus the ratio of the contributions is

$$\frac{\langle \hat{\mathbf{z}} \times \mathbf{J}_v \rangle_{\text{bound}}}{\langle \hat{\mathbf{z}} \times \mathbf{J}_v \rangle_{\text{free}}} \approx \frac{1}{2\pi} r_c^2 \frac{\tilde{n}_f^2}{n_f} \leq \frac{1}{2\pi} r_c^2 \tilde{n}_f \tag{A10}$$

AHNS,[1] Eq. (4.19) gives for $\tilde{n}_f$

$$\tilde{n}_f \sim \frac{2x_0(T)}{a_0^2}\left(\frac{a_0}{r_c}\right)^{2+x_0(T)} \tag{A11}$$

with $x_0(T)$ as in Eq. (18). Thus we finally have

$$\frac{\langle \hat{\mathbf{z}} \times \mathbf{J}_v \rangle_{\text{bound}}}{\langle \hat{\mathbf{z}} \times \mathbf{J}_v \rangle_{\text{free}}} \sim 2x_0(T)\left(\frac{a_0}{r_c}\right)^{x_0(T)} \tag{A12}$$

which should be small for small experimental values of v_s.

APPENDIX B

In this Appendix we show that, within our model, the neglect of free vortices due to escape over the potential barrier in our thermal resistivity calculation of Section 3 was justified. Equation (34) upon setting $n_f = 0$ gives an upper bound on the velocity v_s,

$$v_s \leq \frac{s_g \nabla T}{\rho_0 24\eta/\rho_g^2 d^3} \tag{B1}$$

Using $s_g \simeq 2\times 10^8$ erg/g K given by the ideal gas relation,[19] estimating $\rho_0 \simeq 5\times 10^{-9}$ g/cm^2 by using the bulk density times the number of fluid layers (approximately one atomic layer of helium is believed to solidify on the substrate), using the value $24\eta/\rho_g^2 d^3 \simeq 10^{17}$ and the measured value $\nabla T \simeq 10^{-3}$ K/cm, we obtain

$$v_s \lesssim 5\times 10^{-4} \text{ cm/sec} \tag{B2}$$

and a critical separation

$$r_c \gtrsim 0.3 \text{ cm} \tag{B3}$$

Above T_c, the criterion $\xi_+ \simeq r_c$ sets in at about $T \simeq 1.43$ K ($\simeq 6$ m K above T_c), which, as we see from Fig. 4, is still in the gas-dominated region. Below T_c we can use (38) to estimate the density of such free vortices. We find $n_f \simeq 10/\text{cm}^2$, which, by criterion (35), is far too few to be seen.

Experimentally there is an additional observation arguing against the significant presence of such free vortices. To the extent that such free vortices are present, they would effect the Q^{-1} of the torsional oscillator as well as the thermal resistivity. A separate experimental run was made with the heater turned off and hence with no steady v_s along the axis of rotation and so no possibility of free vortices due to escape over a potential barrier. The Q^{-1} curve thus produced did not differ significantly from the Q^{-1} curve with the heater on (in particular the widths of the Q^{-1} peaks were the same).

Recently[27] there has been some work suggesting that screening of the vortex pair interaction by free vortices may significantly reduce the critical separation locating the potential barrier from the estimate of AHNS. If so, above T_c, where we have many free vortices due to thermal activation, we might find the escape of pairs over the potential barrier continuing to contribute to n_f at higher temperatures above T_c than we have estimated in this Appendix. If so, it may be possible to reduce the present discrepancy between theory and experiment in the transition region.

ACKNOWLEDGMENTS

I would like to thank G. Agnolet and J. Reppy for generously allowing me to use some of their preliminary heat conduction data as well as for many valuable discussions. I would also like to thank V. Ambegaokar and D. Nelson for helpful conversations and advice.

REFERENCES

1. V. Ambegaokar, B. I. Halperin, D. R. Nelson, and E. D. Siggia, *Phys. Rev. B* **21**, 1806 (1980).
2. J. M. Kosterlitz and D. J. Thouless, *J. Phys. C* **6**, 1181 (1973).
3. J. M. Kosterlitz, *J. Phys. C* **7**, 1046 (1974).
4. D. R. Nelson and J. M. Kosterlitz, *Phys. Rev. Lett.* **39**, 1201 (1977).
5. D. J. Bishop and J. D. Reppy, *Phys. Rev. B* **22**, 5171 (1980).
6. D. Bergman, *Phys. Rev.* **188**, 370 (1969).
7. D. Bergman, *Phys. Rev. A* **3**, 2058 (1971).
8. H. J. Verbeek, Ph.D. Thesis, University of Leiden (1980).
9. T. G. Wang and I. Rudnick, *J. Low Temp. Phys.* **9**, 425 (1972).
10. I. Rudnick, R. S. Kagiwada, J. C. Fraser, and E. Gruyon, *Phys. Rev. Lett.* **20**, 430 (1968).
11. I. Rudnick and J. C. Fraser, *J. Low Temp. Phys.* **3**, 225 (1970).
12. B. I. Halperin, in *Proc. Kyoto Summer Institute on Low Dimensional Systems* (Research Institute for Fundamental Physics, Kyoto, 1979).
13. I. Rudnick, *Phys. Rev. Lett.* **40**, 1454 (1978).
14. B. Ratnam and J. Mochel, *J. Low Temp. Phys.* **3**, 239 (1970).
15. B. Ratnam and J. Mochel, in *Low Temperature Physics—LT 13*, Timmerhaus, O'Sullivan, and Hammel, eds. (Plenum, New York, 1979), Vol. 1, p. 233.

16. J. E. Rutledge, Ph.D. Thesis, University of Illinois (1978).
17. S. Teitel, Ph.D. Thesis, Cornell University (1981).
18. L. D. Landau and E. M. Lifshitz, *Fluid Mechanics* (Pergamon Press, London, 1959), p. 56.
19. F. Reif, *Fundamentals of Statistical and Thermal Physics* (McGraw-Hill, New York, 1965).
20. H. Højgaard Jensen, H. Smith, P. Wölfe, K. Nagai, and T. Maack Bisgaard, *J. Low Temp. Phys.* **41**, 473 (1980).
21. G. Agnolet and J. D. Reppy, private communication.
22. M. Bienfait, J. G. Dash, and J. Stoltenberg, *Phys. Rev. B* **21**, 4624 (1980).
23. G. B. Hess, R. J. Muirhead, and J. G. Dash, unpublished.
24. J. Maps and R. B. Hallock, to be published.
25. V. Ambegaokar and S. Teitel, *Phys. Rev. B* **19**, 1667 (1979).
26. J. L. McCauley, *J. Phys. C* **10**, 689 (1977).
27. Lu Yu, Phys. Rev. *B* **23**, 3569 (1981).
28. G. Agnolet, S. Teitel, and J. D. Reppy, to be published.